Location of a Constriction in the Lumen of a Transmembrane Pore by Targeted Covalent Attachment of Polymer Molecules

Liviu Movileanu,* Stephen Cheley,* Stefan Howorka,* Orit Braha,* and Hagan Bayley*‡

From the *Department of Medical Biochemistry and Genetics, The Texas A&M University System Health Science Center, College Station, Texas 77843; and ‡Department of Chemistry, Texas A&M University, College Station, Texas 77843

ABSTRACT Few methods exist for obtaining the internal dimensions of transmembrane pores for which 3-D structures are lacking or for showing that structures determined by crystallography reflect the internal dimensions of pores in lipid bilayers. Several approaches, involving polymer penetration and transport, have revealed limiting diameters for various pores. But, in general, these approaches do not indicate the locations of constrictions in the channel lumen. Here, we combine cysteine mutagenesis and chemical modification with sulfhydryl-reactive polymers to locate the constriction in the lumen of the staphylococcal α-hemolysin pore, a model protein of known structure. The rates of reaction of each of four polymeric reagents (MePEG-OPSS) of different masses towards individual single cysteine mutants, comprising a set with cysteines distributed over the length of the lumen of the pore, were determined by macroscopic current recording. The rates for the three larger polymers (1.8, 2.5, and 5.0 kD) were normalized with respect to the rates of reaction with a 1.0-kD polymer for each of the seven positions in the lumen. The rate of reaction of the 5.0-kD polymer dropped dramatically at the centrally located Cys-111 residue and positions distal to Cys-111, whether the reagent was applied from the trans or the cis side of the bilayer. This semi-quantitative analysis sufficed to demonstrate that a constriction is located at the midpoint of the pore lumen, as predicted by the crystal structure, and although the constriction allows a 2.5-kD polymer to pass, transport of a 5.0-kD molecule is greatly restricted. In addition, PEG chains gave greater reductions in pore conductance when covalently attached to the narrower regions of the lumen, permitting further definition of the interior of the pore. The procedures described here should be applicable to other pores and to related structures such as the vestibules of ion channels.

KEY WORDS: α-hemolysin • pore • cysteine scanning mutagenesis • sulfhydryl reagent • poly(ethylene glycol)

INTRODUCTION

Protein pores allow molecules of several hundred daltons or more to pass through biological membranes. Examples include the outer membrane porins of gram-negative bacteria, pore-forming toxins, and components of the immune system such as perforin and the membrane–attack complex of complement. Various techniques have been used to measure the effective diameters of pores in the absence of structural information. Efforts to measure internal geometry, including the sites of internal constrictions, have been more limited because of the technical difficulty of this task.

Experimental approaches to the determination of the pore diameter have included single channel recording. Many pores exhibit roughly ohmic behavior and, in this case, the unitary conductance can be translated into a pore diameter by making simplifications, notably the assumption of a cylindrical geometry (Menestrina, 1986; Hille, 1992; Korchev et al., 1995). In a second approach, the interactions of water-soluble polymers and other large molecules with pores have been examined. Two types of measurements can be made: (1) the ability of a polymer to penetrate into the lumen of a pore; and (2) the ability of a polymer to be transported across the bilayer by a pore. If the geometry of a pore were cylindrical, these approaches would give similar results. However, cylindrical geometry cannot be assumed, and penetration and transport must be distinguished.

The ability of polymers to penetrate pores can be manifested by the reductions in conductance brought about by polymer within the pore (Krasilnikov et al., 1992) or changes in access resistance, the ability of the adjacent electrolyte to feed ions to the entrance of a pore (Vodyanoy and Bezrukov, 1992; Bezrukov and Vodyanoy, 1993). Penetration of polymers into the lumen of a pore is also apparent as single channel noise (Bezrukov and Vodyanoy, 1993; Bezrukov et al., 1994; Bezrukov, 2000). The noise may be enhanced by interactions with the wall of the lumen (Bezrukov et al., 1996; Bezrukov and Kasianowicz, 1997). Techniques other than electrical recording are available to deter-

Address correspondence to Dr. Hagan Bayley, Department of Medical Biochemistry and Genetics, The Texas A&M University System Health Science Center, 440 Reynolds Medical Building, College Station, TX 77843-1114. Fax: (979) 847-9481; E-mail: bayley@tamu.edu

mine the penetration of molecules into pores. For example, the ability of a large molecule to enter a pore and quench a fluorescent dye located inside it can be measured (Hamman et al., 1997).

Transport assays with large molecules include measurements of the ability of fluorescent dyes or radiolabeled molecules to pass through pores (Scherrer and Gerhardt, 1971; Füssle et al., 1981; Schwab et al., 1994; Bevans et al., 1998). The translocation of nucleic acids through pores in a transmembrane potential can be verified by PCR, but more readily inferred from current recordings (Kasianowicz et al., 1996). In one case, the diameter of the pore was revealed by the ability to transport single-stranded but not double-stranded DNA (Kasianowicz et al., 1996). In other cases, double-stranded DNA appears to be transported (Szabò et al., 1997, 1998). The failure of a polymer to be transported can also be revealed by osmotic effects with assays such as red cell lysis and liposome swelling (Decad and Nikaido, 1976; Colombini, 1980; Palmer et al., 1993; Fajardo et al., 1998).

An attractive means to define the internal geometry of pores has been investigated by Krasilnikov and colleagues who have determined the diameters of both entrances and the sites of constrictions in the voltage-dependent anion channel (Carneiro et al., 1997), colicin Ia (Krasilnikov et al., 1998), and staphylococcal α-hemolysin (αHL;[1] Merzlyak et al., 1999) by analyzing the unitary conductance before and after application of a penetrating polymer to one side of the bilayer and a nonpenetrating polymer to the other side. The site of binding of a rigid macromolecule, β-cyclodextrin, in the αHL pore has been inferred from the results of mutagenesis studies (Gu et al., 1999).

Here, we introduce an approach that combines cysteine mutagenesis and chemical modification (Akabas et al., 1992; Krishnasastry et al., 1994; Holmgren et al., 1996; Horn, 1998; Karlin and Akabas, 1998) with the use of polymeric reagents (Holz and Finkelstein, 1970; Scherrer and Gerhardt, 1971; Decad and Nikaido, 1976; Colombini, 1980). Recently, we showed that a single PEG molecule covalently tethered inside the αHL pore produces a substantial reduction in unitary conductance (Howorka et al., 2000; Movileanu et al., 2000). Therefore, the stage was set to test our approach by targeted modification of cysteine mutants of αHL. αHL is a 293-residue polypeptide, which assembles in lipid bilayers to form a mushroom-shaped heptameric transmembrane pore (Song et al., 1996). There are two distinct regions of the lumen of the assembled protein (see Fig. 1). On the cis side, the protein contains a large cavity, which measures ~46 Å in internal diameter and is entirely located within the extramembranous domain. In the transmembrane domain, the channel lumen narrows to form a 14-stranded β-barrel with an average internal diameter of ~20 Å. In the crystal structure, the two domains are separated by a constriction with a diameter of ~14 Å (see Fig. 1).

In our approach, the rates of reaction of each member of a set of four polymeric reagents with individual single cysteine mutants were determined by macroscopic current recording. The cysteines were distributed along the length of the lumen of the pore. A semi-quantitative analysis sufficed to demonstrate that the constriction is at the midpoint of the pore lumen, near residue 111 as predicted by the crystal structure, and restricts the passage of a PEG of 5.0 kD, but not a PEG of 2.5 kD. The relatively low concentrations of polymers used here obviate some of the problems associated with higher concentrations including effects on solution conductivity and ion activity, osmotic stress on the protein under investigation, and the relatively poor understanding of polymer properties in the "semi-dilute" regime. The procedure should be applicable to other pores and to related structures such as the vestibules of ion channels.

MATERIALS AND METHODS

Cysteine Scanning Mutagenesis

Single cysteine mutants were constructed by cassette mutagenesis using a reconstructed αHL gene in a T7 vector (pT7-αHL-RL2; Cheley et al., 1999). The αHL-RL2 gene features 10 unique restriction sites that span codons 103–158, which allows convenient mutagenesis of the β-barrel and triangle regions of the αHL pore. To construct the mutant S106C, pT7-αHL-RL2 was digested with SacII and HpaI, and the resulting internal sequence was replaced with duplex DNA prepared from 5′-GGAATTGCATTGATACAAAAGAGTATATGAGTACGCT-3′ (sense) and 5′-AGCGTACTCATATACTCTTTTGTATCAATGCAATTCCGC-3′ (antisense). The cysteine codon is underlined. Before sequence verification, plasmids were screened by digestion with HpaI. This restriction site is present in the αHL-RL2 gene but absent from S106C DNA. Another single cysteine mutant, M113C, was constructed by using a similar strategy. pT7-αHL-RL2 was digested with SacII and HpaI, and the internal fragment was replaced with duplex DNA prepared from 5′-GGAATTCGATTGATACAAAAGAGTATTGCAGTACGTT-3′ (sense) and 5′-AACGTACTGCAATACTCTTTTGTATCAATCGAATTCCGC-3′ (antisense). To construct T117C, pT7-αHL-RL2 was digested with HpaI and BstEII, and the internal fragment was replaced with duplex DNA prepared from 5′-ATGTTACGGATTCAACG-3′ (sense) and 5′-GTTACCGTTGAATCCGTAACAT-3′ (antisense). An internal BsiWI site that is present in the αHL-RL2 gene but absent in T117C DNA was used to screen for cassette replacement before DNA sequencing. To construct L135C, pT7-αHL-RL2 was digested with SpeI and ApaI, and the internal fragment was replaced by the cassette prepared from 5′-CTAGTAAAATTGGAGGGTGTATTGGGGCC-3′ (sense) and 5′-CCAATACACCCTCCAATTTTA-3′ (antisense). A StuI site present in the αHL-RL2 gene but absent in L135C DNA was used for screening before DNA sequencing. Mutants K8C, E111C, and T129C were also used in the present study and had been constructed previously (Walker and Bayley, 1995). All mutants were verified by sequencing the entire αHL gene.

[1]*Abbreviation used in this paper:* αHL, staphylococcal α-hemolysin.

Homoheptamer Formation and Purification

For bilayer experiments, mutant αHL polypeptides were synthesized in vitro by coupled transcription and translation and assembled into homoheptamers by the inclusion of rabbit red cell membranes during synthesis as previously described (Cheley et al., 1999). To protect cysteine residues from oxidation, the procedure was modified as follows. A suspension of rabbit red blood cell membranes (20 μl, 1 mg/ml) was diluted with MBSA buffer (500 μl of 10 mM MOPS, 150 mM NaCl, pH 7.4, titrated with NaOH, containing 1 mg/ml BSA). The membranes were spun down (for 5 min at 21,000 *g*) and the supernatant was removed. The washed membrane pellet was resuspended in a translation mix (100 μl) containing 16 μl of mutant DNA (400 μg/ml), 40 μl premix, 10 μl complete amino acid mix, 30 μl S30 extract (No. L114A; Promega) and 4 μl of [^{35}S]methionine (1,200 Ci/mmol; Amersham Pharmacia Biotech). After 1 h at 37°C, the membranes were pelleted (for 5 min at 21,000 *g*), resuspended in MBSA containing 2 mM DTT (500 μl), and recovered by centrifugation. The washed membrane pellet containing the assembled mutant heptamer was solubilized in 50 μl of sample buffer containing 715 mM β-mercaptoethanol (without heating) and applied to one lane of an 8% SDS–polyacrylamide gel (Laemmli, 1970). The cathode buffer contained 0.1 mM sodium thioglycolate. After overnight electrophoresis, the untreated gel was dried under vacuum at 50°C onto Whatman 3MM paper and exposed to an X-ray film for 1 h. The gel slice containing mutant heptamer was excised using the autoradiogram as the template and rehydrated in a 1.5-ml microcentrifuge tube with 10 mM Tris-HCl, pH 7.5, containing 2 mM DTT (400 μl). After removing the paper backing with flamed forceps, the gel slice was crushed with a disposable plastic pestle. The tube was sealed with parafilm and the mix was rotated overnight at 4°C. Gel fragments were removed from the eluted protein by centrifugation through a 0.2-μm cellulose acetate spin filter (microfilterfuge tube No. 7016-024; Rainin). The recovered filtrate containing the gel-purified homoheptamer (~0.2 μg/ml) was stored in 50-μl aliquots at −80°C.

Polymeric Sulfhydryl Reagents

The following water-soluble polymeric sulfhydryl reagents were used without further purification: monomethoxypoly(ethylene glycol)-*o*-pyridyl disulfide (MePEG-OPSS) 1.0 kD (Lot No. ZF-059-03), 1.8 kD (Lot No. ZF-059-01), 2.5 kD (Lot No. ZF-059-02), and 5.0 kD (Lot No. PT-047-04) (all from Shearwater Polymers Inc.). The number average (M_n) and weight average (M_w) molecular masses of the reagents were determined by gel permeation chromatography. The ratio M_w/M_n is a measure of the mass distribution of a polymer. The masses (M_n) of the MePEG-OPSS reagents were as follows: MePEG-OPSS-1k, 970 D (M_w/M_n = 1.02); MePEG-OPSS-1.8k, 1,810 D (M_w/M_n = 1.02); MePEG-OPSS-2.5k, 2,530 D (M_w/M_n = 1.03); and MePEG-OPSS-5k, 5,030 D (M_w/M_n = 1.02). Aqueous stocks of 100 mM MePEG-OPSS were stored in portions of 50 μl at −20°C.

The purity and homogeneity of the MePEG-OPSS reagents were determined by modifying a radiolabeled monomeric cysteine mutant of αHL (K8C), followed by analysis of the products by SDS-PAGE and quantitative autoradiography (Howorka et al., 2000). PEG-modified monomeric αHL migrates more slowly than the unmodified protein in SDS gels. Hence, the extent of modification by MePEG-OPSS could be determined. All four MePEG-OPSSs modified between 90 and 95% of K8C. This high extent of modification indicates the absence of sulfhydryl-reactive impurities, such as 2,2′-dipyridyl disulfide, which is used for the synthesis of the MePEG-OPSSs (Woghiren et al., 1993). αHL mutants blocked by this impurity would comigrate with unmodified αHL and lower the apparent extent of modification. The absence of impurities was also shown by TLC using precoated, fluorescent silica plates (No. 5719-2; Merck) eluted with ethyl acetate/acetone/water (1:10:2).

The mass distribution of the polymer in the MePEG-OPSSs was assessed from the broadening of the gel bands of MePEG-modified αHL K8C. The bands were only slightly broadened, indicating that the molecular size distribution of all four of the MePEG polymers is narrow as suggested by the M_w/M_n ratios determined by gel permeation chromatography. The pK_a of the pyridyl group in MePEG-OPSS was determined by measuring the absorption of a 0.1-mM solution of MePEG-OPSS-1k between 230 and 400 nm. The absorbance at 300 nm was plotted versus pH, while titrating over the range pH 1.0–9.0 by the addition of 0.1 M HCl or 0.1 M NaOH. The pK_a value derived from the midpoint of the transition was 2.0. By comparison, the value for monoprotonated 2,2′-dipyridyl disulfide is pK_a = 2.45 (Brocklehurst and Little, 1973).

Planar Bilayer Recordings

Macroscopic (multichannel) current measurements were carried out with planar lipid membranes (Montal and Mueller, 1972; Braha et al., 1997; Howorka et al., 2000). In brief, the A and B chambers (2 ml each) of the bilayer apparatus were separated by a 25-μm thick Teflon septum (Goodfellow Corporation). An aperture in the septum of ~150 μm diam was pretreated with hexadecane (Sigma-Aldrich) dissolved in highly purified n-pentane (Burdick and Jackson; Allied Signal Inc.) at a concentration of 10% (vol/vol). The electrolyte in both chambers was 300 mM KCl, 5 mM Tris-HCl, pH 8.5, containing 100 μM EDTA and 200 μM DTT. The bilayer was formed with 1,2-diphytanoyl-sn-glycerophosphocholine (Avanti Polar Lipids Inc.). Bilayer formation was monitored by the increase in the membrane capacitance to a final value of 120–160 pF. αHL was added to the B chamber, and the A chamber was at ground. As in previous papers, the cis entrance to the protein is in the cap, and the trans entrance is in the transmembrane β barrel (see Fig. 1). A potential of −40 mV at the trans entrance with respect to the cis entrance was maintained in all the experiments described here. Current flow is shown as positive and represents the positive charge moving from the B to the A chamber (i.e., from the cis entrance to the trans entrance of the pore). This current convention is opposite, with respect to the protein, to our previous papers. Measurements were performed at 23 ± 0.5°C.

The insertion of αHL pores into the bilayer was performed by adding gel-purified homoheptamers (5–20 μl) to the B chamber to give a final protein concentration of 0.5 to 2 ng/ml. The B solution was stirred for 35–60 min until a steady multichannel current was obtained. Experiments were performed only if at least 20 channels inserted into the lipid bilayer. Currents were recorded by using a patch-clamp amplifier (model Axopatch 200B; Axon Instruments) connected to the chambers by Ag/AgCl electrodes, and monitored by a two-channel oscilloscope (model TAS250; Tektronix). The current traces were low-pass filtered with a built-in 4-pole Bessel filter at a frequency of 5 kHz and stored using a digital audio tape recorder (DAS-75; Dagan Corp.). A Pentium PC equipped with a DigiData 1200 A/D converter (Axon Instruments) was used for data acquisition. For computer analysis, the data was further filtered by an 8-pole Bessel filter (model 900; Frequency Devices) at a frequency of 100 Hz and sampled at 1 kHz. For display and further manipulation of the current traces, we used pCLAMP8 (Axon Instruments) and Origin6 (Microcal Software) after additional filtering at 30 Hz.

Apparent Rate Constants

We examined the reaction kinetics of seven cysteine mutants: five mutations were located in the β barrel and the other two in the

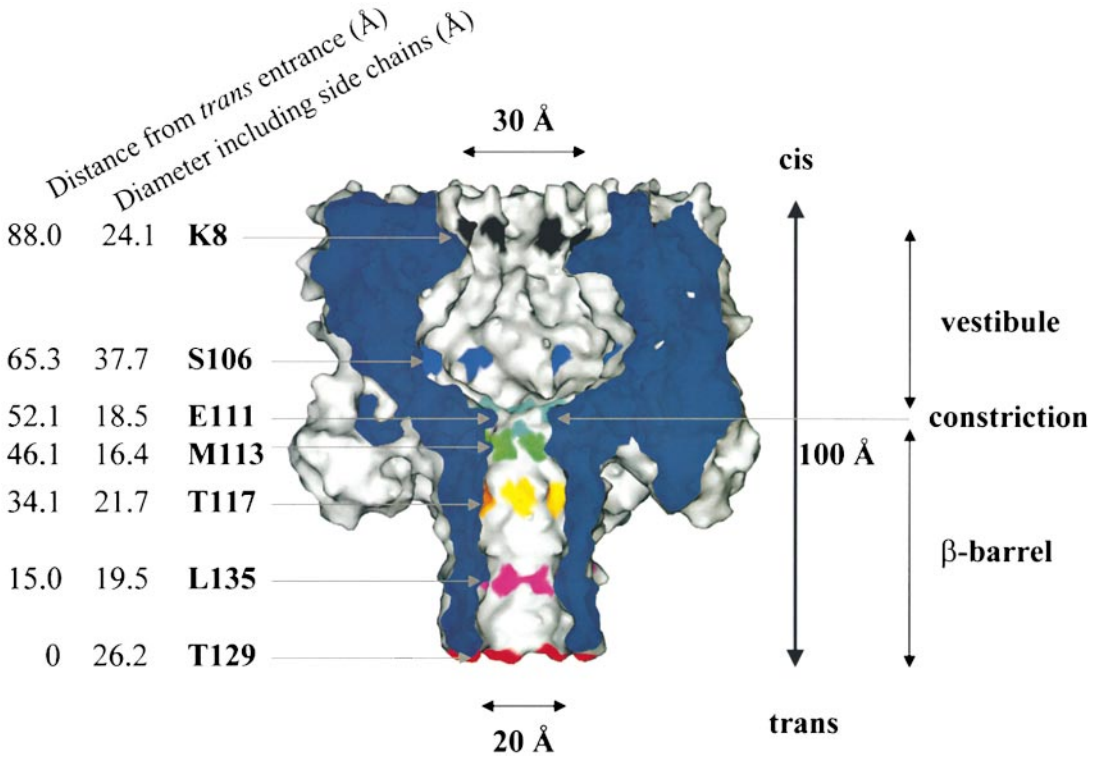

FIGURE 1. Sagittal section through the heptameric αHL pore. The seven sites of cysteine substitution are indicated with their distances from the trans entrance. The internal diameters of the wild-type pore at the sites of substitution are also shown. The figure and dimensions were generated from crystallographic data (Song et al., 1996) with the SPOCK software package (Christopher, 1998). The internal diameters were generated by fitting a circle to the coordinates of the C, N, or O terminal atoms of the amino acid side chains. For positions 8, 106, and 111, a few amino acid sidechains, which were oriented away from the molecular sevenfold axis, were ignored. In each of these cases, the circles were fitted to the terminal atoms of the remaining side chains, which were in the same plane.

cavity (see Fig. 1). Taking into account the four polymeric reagents, and the two sites of application (chambers A and B, which are contacted by the trans and cis sides of the protein, respectively), there are 56 distinct experiments required to determine the reaction rates of the water-soluble PEG reagents at the different sites in the lumen of the pore. The values in this paper are means ± SD for at least four experiments under each condition. 4 mM MePEG-OPSS was added to either the A or B chamber with continuous stirring at 700 rpm. The slightly alkaline pH of 8.5 was chosen to increase the extent of ionization of the cysteine residues and thereby increase their reaction rates. For instance, with the mutant pore $M113C_7$ or $T129C_7$, reaction was hardly detectable at pH 7.0, even with MePEG-OPSS-1k. No change in the pH of the chamber occurred after addition of a polymeric reagent.

Once the macroscopic current remained unchanged, signifying that a reaction was complete, unreacted MePEG-OPSS was washed out of the chamber with a peristaltic pump. Finally, 10 mM DTT was added to both chambers to cleave the PEG chains from the protein and demonstrate that the unmodified pore could be regenerated. Stirring in both chambers was maintained at 700 rpm during the cleavage step. The time required for a complete experiment was 40–80 min.

The apparent first-order rate constants (k′) for reaction of the MePEG-OPSS reagents with cysteine sulfhydryls were determined by fitting the macroscopic current decays to the following exponential function (Pascual and Karlin, 1998):

$$I_t = I_\infty - (I_\infty - I_0)\exp(-k't), \quad (1)$$

where the subscripts indicate the time at which the macroscopic current was measured, I_0 and I_∞ represent the currents corresponding to the beginning and end of the reaction, and t de-

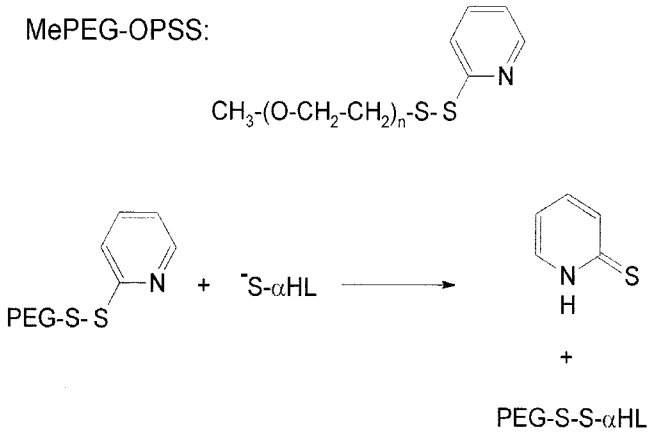

FIGURE 2. Sulfhydryl-directed polymeric reagents used in this study. (Top) MePEG-OPSS reagents. MePEG-OPSS-1k, $n \approx 19$; MePEG-OPSS-1.8k, $n \approx 39$; MePEG-OPSS-2.5k, $n \approx 56$; and MePEG-OPSS-5k, $n \approx 113$. (Bottom) The reagents react with free sulfhydryl groups. The MePEG is attached through a disulfide linkage and 2-thiopyridone is released.

TABLE I

Apparent First-order Reaction Rate Constants (k′, s^{-1}) for the Reactions of MePEG-OPSS Reagents from the Trans Side of the Pore

	αHL cysteine mutant						
MePEG-OPSS	$T129C_7$	$L135C_7$	$T117C_7$	$M113C_7$	$E111C_7$	$S106C_7$	$K8C_7$
kD							
1.0	0.043 ± 0.002	0.24 ± 0.05	1.2 ± 0.1	0.027 ± 0.002	0.64 ± 0.06	0.046 ± 0.002	0.19 ± 0.04
1.8	0.016 ± 0.002	0.083 ± 0.003	0.35 ± 0.03	0.0091 ± 0.0019	0.16 ± 0.02	0.0093 ± 0.0007	0.0045 ± 0.0006
2.5	0.0076 ± 0.0011	0.028 ± 0.002	0.19 ± 0.02	0.0032 ± 0.0008	0.046 ± 0.002	0.0036 ± 0.0005	0.0015 ± 0.0003
5.0	0.00086 ± 0.00036	0.0024 ± 0.0006	0.0072 ± 0.0014	0.00025 ± 0.00011	<0.00024	<0.00024	<0.00024

Current traces were fitted to an exponential function as described in MATERIALS AND METHODS. Coefficient of determination (R^2) values were between $R^2 = 0.96$ and 0.99. The k′ values for $L135C_7$, $T117C_7$, $M113C_7$, and $E111C_7$ represent rate constants for reaction at one of the seven available sulfhydryls. For $T129C_7$ and $K8C_7$, and $S106C_7$ with MePEG-OPSS-1k, the macroscopic current decays could be fitted by single exponentials resulting in composite k′ values for these cases where >1 MePEG becomes attached. The k′ values are not corrected for the statistical effect arising from the presence of seven identical subunits at the start of the reaction.

notes the cumulative time of the reaction. The rate of reaction of a MePEG-OPSS with cysteine sulfhydryls is given by:

$$v = kc_{PEG}n_s = k'n_s, \quad (2)$$

where k is the second-order reaction rate constant, n_S is the number of reactive cysteine sulfhydryls, and c_{PEG} is the concentration of polymeric reagent in the lumen of the pore. For most cases, the decay of the macroscopic current (I_t) with time (t) could be fitted to a single exponential function yielding values for k′ and I_∞. The coefficient of determination (R^2) values were between 0.96 and 0.99. In the case of $T117C_7$ and MePEG-OPSS-1k, the reaction was biphasic and I_∞ for the first phase was determined as described in the text. Here, fitting of the early part of the time course revealed k′ for the reaction of MePEG-OPSS-1k with the first sulfhydryl residue of the seven.

RESULTS

Experimental Design

We examined the reaction of MePEG-OPSS reagents with cysteines located at various positions throughout the lumen of the αHL pore (Fig. 1). The homoheptameric mutant pores each contained seven cysteine residues. The reagents had the following masses: 1.0, 1.8, 2.5, and 5.0 kD. The MePEG-OPSSs react with cysteine sulfhydryls leaving a monomethoxy–PEG chain attached to the protein through a disulfide linkage (Fig. 2). Under the conditions of the experiments, pH = 8.5, the reagents are neutral since the OPSS group has $pK_a = 2.0$, as determined by titration and spectrophotometry. The applied potential was the same for all the reactions described here, i.e., −40 mV at the trans entrance of the lumen with respect to the cis entrance.

Rates of Reaction of MePEG-OPSS Reagents with Cysteine Mutants of αHL

The apparent first-order rate constants (k′) for the reaction of the MePEG-OPSS reagents with the cysteine sulfhydryls could be measured over four orders of magnitude (Tables I and II). The rates of reaction depended on the side of application, the mass of the reagent, and the position of the mutation. For example, when MePEG-OPSS-1k was applied from the trans side, k′ varied by two orders of magnitude when the different positions within the lumen of the pore were compared (Fig. 3 A). The most reactive cysteines were in $T117C_7$ and $E111C_7$ (Fig. 3 A), with $k' = 1.2 \pm 0.1\ s^{-1}$ ($n = 4$) and $0.64 \pm 0.06\ s^{-1}$ ($n = 4$), respectively, for MePEG-OPSS-1k (Table I). The least reactive cysteines were in $T129C_7$ and $M113C_7$ (Fig. 3 A), with $k' = 0.043 \pm 0.002\ s^{-1}$ ($n = 5$) and $0.027 \pm 0.002\ s^{-1}$ ($n = 4$), respectively, for MePEG-OPSS-1k (Table I).

In another example, the time courses of reaction with all four MePEG-OPSSs from the cis side with a sin-

TABLE II

Apparent First-order Reaction Rate Constants (k′, s^{-1}) for the Reactions of MePEG-OPSS Reagents from the Cis Side of the Pore

	αHL cysteine mutant						
MePEG-OPSS	$T129C_7$	$L135C_7$	$T117C_7$	$M113C_7$	$E111C_7$	$S106C_7$	$K8C_7$
kD							
1.0	0.035 ± 0.002	0.080 ± 0.004	1.0 ± 0.1	0.024 ± 0.002	0.60 ± 0.06	0.021 ± 0.002	0.50 ± 0.07
1.8	0.0029 ± 0.0009	0.0070 ± 0.0012	0.34 ± 0.06	0.0076 ± 0.0014	0.21 ± 0.05	0.0081 ± 0.0011	0.22 ± 0.04
2.5	0.00091 ± 0.00020	0.0037 ± 0.0005	0.038 ± 0.003	0.0019 ± 0.0003	0.11 ± 0.04	0.0042 ± 0.0018	0.080 ± 0.019
5.0	<0.00024	<0.00024	<0.00024	<0.00024	<0.00024	0.00032 ± 0.00023	0.0094 ± 0.0009

See Table I legend for details.

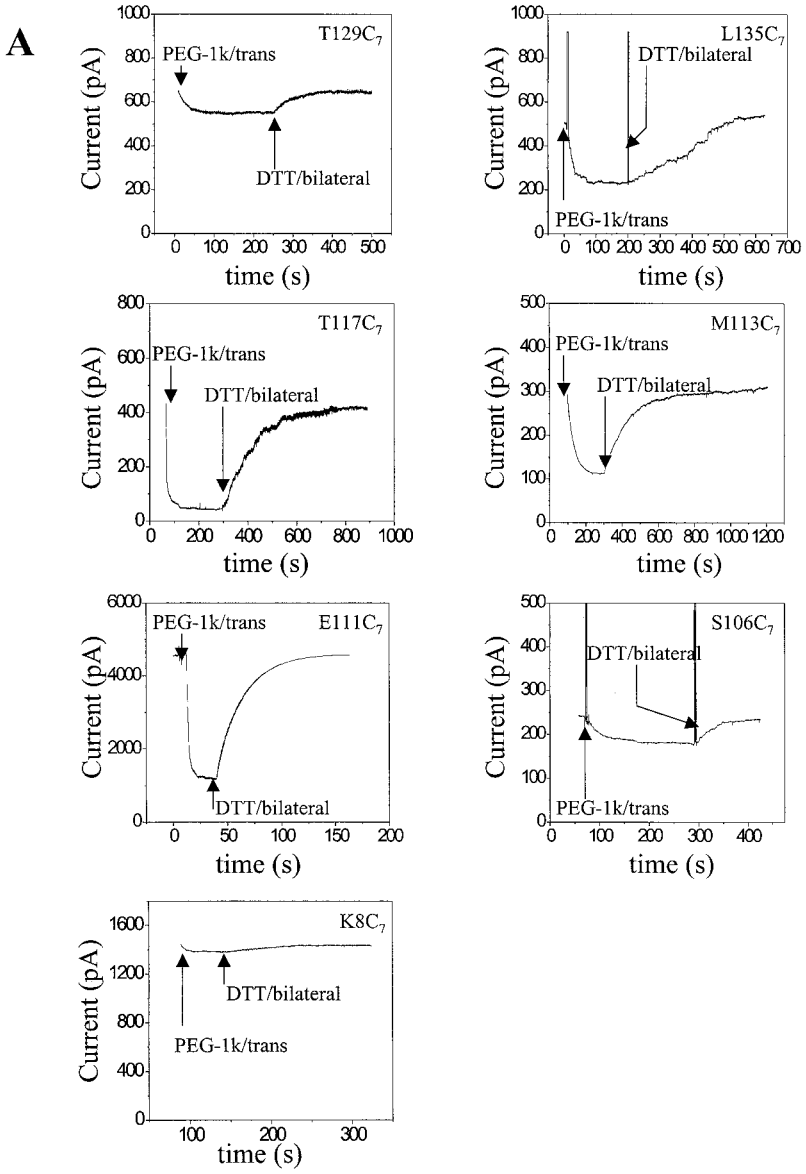

FIGURE 3. Examples of reaction time courses for MePEG-OPSS reagents with αHL cysteine mutants. αHL homoheptamers were purified by electrophoresis and allowed to insert into planar bilayers to give macroscopic currents (>20 pores). The applied potential was −40 mV. The signal was filtered with a low-pass Bessel filter at 100 Hz. The decrease in current was monitored after the addition of 4 mM MePEG-OPSS reagent at pH 8.5. After a new steady current level was reached, the MePEG was cleaved from the protein with DTT. (A) Reaction time courses for all seven mutated sites with one reagent (MePEG-OPSS-1k) applied from the trans side. (B) Reaction time courses at a single site (T129C) with all four polymeric reagents (MePEG-OPSS-1k, MePEG-OPSS-1.8k, MePEG-OPSS-2.5k, and MePEG-OPSS-5k) applied from the cis side. (C) Reaction time courses for a single site (T117C) with a single reagent (MePEG-OPSS-5k) applied from either the trans or the cis side.

gle mutant, $T129C_7$, are shown (Fig. 3 B and Table II). We observed no change in the macroscopic current when MePEG-OPSS-5k was added to the cis side. The lowest measurable rate would be 0.00024 s^{-1}, for a 1% change in current per minute and a I_∞/I_0 value of 0.3. However, a very slow change of the current was recorded with MePEG-OPSS-2.5k, $k' = 0.00091 \pm 0.00020\ s^{-1}$ ($n = 4$). The fastest reaction was with MePEG-OPSS-1k, $k' = 0.035 \pm 0.002\ s^{-1}$ ($n = 4$).

In a final example, the reaction of single reagent, MePEG-OPSS-5k, with $T117C_7$ from both the trans and cis sides of the pore are compared (Fig. 3 C). When MePEG-OPSS-5k is applied from the trans side, the reaction is rapid with $k' = 0.0072 \pm 0.0014\ s^{-1}$ ($n = 7$). By contrast, no reaction is seen when MePEG-OPSS-5k is applied from the cis side reaction. As noted above, this implies that $k' \leq 0.00024\ s^{-1}$.

With the exception of T117C with MePEG-OPSS-1k (see next paragraph), the rates of reaction of the cysteines in the β barrel (L135C, T117C, M113C, and E111C) with the MePEG-OPSS reagents represent the reaction of one sulfhydryl of the seven that are available. In the cases of $L135C_7$, $M113C_7$, and $E111C_7$, the treatment of the single pores with MePEG-OPSS-1k showed a single step decrease in conductance to a value that was close to the value of I_∞/I_0 obtained from macroscopic currents ($L135C_7$, 38 ± 4%, $n = 3$; $M113C_7$, 33 ± 2%, $n = 3$; and $E111C_7$, 30 ± 2%, $n = 3$). In the case of $S106C_7$, the current steps in single-channel experiments showed that up to three MePEG-OPSS-1k react, but only one molecule of the larger reagents attach in the lumen at this position (data not shown). Further, the I_∞/I_0 values obtained from macroscopic currents were similar to those obtained from pores constructed with a

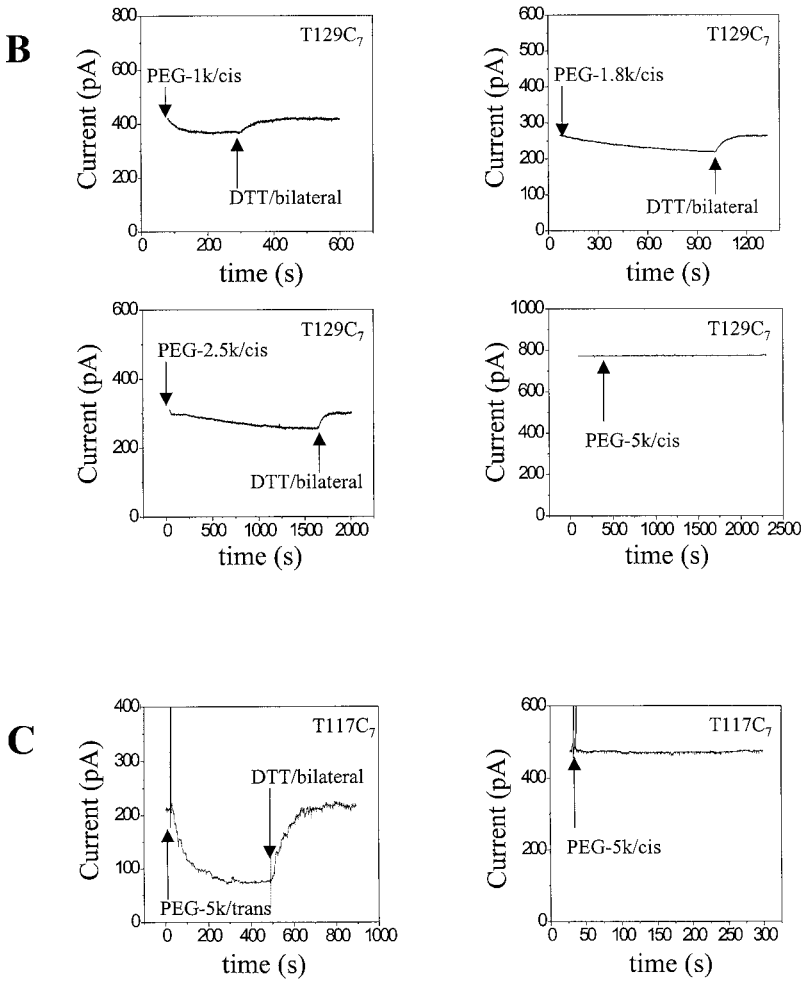

Figure 3 (continued)

single 3.4- or 5.0-kD PEG at position 106 (Howorka et al., 2000), again suggesting that only one of the larger reagents reacts with each $S106C_7$ pore (Movileanu et al., 2000). In the cases of $T129C_7$ and $K8C_7$, all seven cysteines can accommodate the larger MePEG chains (Howorka et al., 2000; Movileanu, L., unpublished results). Therefore, the k′ values for $L135C_7$, $T117C_7$ (see next paragraph), $M113C_7$, and $E111C_7$ represent rate constants for reaction at one of the seven available sulfhydryls. For $T129C_7$ and $K8C_7$, and $S106C_7$ with MePEG-OPSS-1k, the macroscopic current decays could be fitted by single exponentials resulting in composite k′ values for these positions, which only approximate the k′ values for the first cysteines that react.

The Most Reactive Cysteine Mutant, Homoheptamer $T117C_7$, Is Modified by a Second MePEG-1k

In most cases, the reaction with MePEG-OPSS in the αHL barrel followed a single exponential (Fig. 3). However, it was apparent, by inspection of the plot of $-\ln((I_t - I_\infty)/(I_0 - I_\infty))$ versus time, that the reaction between MePEG-OPSS-1k and $T117C_7$ was more complex (Fig. 4 A). The data suggested that MePEG-OPSS-1k reacts with $T117C_7$ on more than one cysteine residue. To confirm this hypothesis, we performed measurements with 10–15 channels in the bilayer, a smaller number than usual (Fig. 4 B). The current trace followed two distinct phases. The first was characterized by a fast stepwise decrease in the current with steps of 5.5 ± 0.1 pA ($n = 55$, in four separate experiments). In the second phase, the rate of decrease of the current was slower and occurred in steps of 2.5 ± 0.2 pA ($n = 51$, in four separate experiments). During the transition between the two phases, both the large and small current steps were seen. These data strongly suggest that two PEGs of 1 kD can react at position 117, the second causing a smaller decrease in current than the first.

A value of $I_\infty/I_0 = 0.31$ obtained from a single-channel experiment was used to fit the first part of the curve for the reaction of MePEG-OPSS-1k with $T117C_7$, yielding $k' = 1.2 \pm 0.1\ s^{-1}$ ($n = 4$) from the trans side and $1.0 \pm 0.1\ s^{-1}$ ($n = 4$) from the cis side. The first part of the cur-

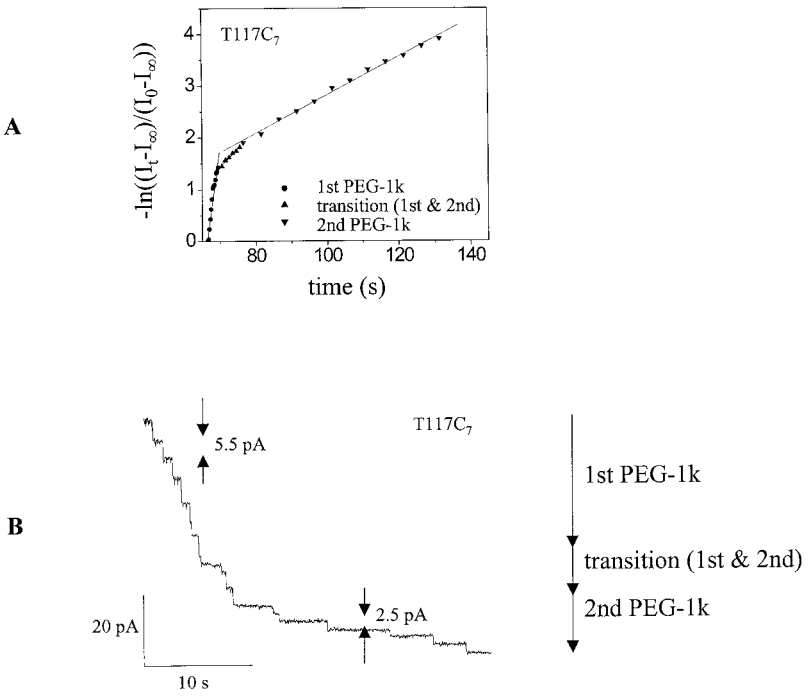

FIGURE 4. MePEG-OPSS-1k reacts sequentially with two cysteines in $T117C_7$. (A) Plot of $-\ln((I_t - I_\infty)/(I_0 - I_\infty))$ versus time, using a value of 43 pA for I_∞ obtained at 100 s (I_0 was 427 pA; see Fig. 3 A). (B) Stepwise decrease in the current arising from ~16 $T117C_7$ pores.

rent decay for reaction from the trans side was also fitted directly to a single exponential function, yielding $k' = 1.1 \pm 0.1\ s^{-1}$ ($n = 4$) and $I_\infty/I_0 = 0.30$. The kinetics of channel block by MePEG-OPSS-1.8k, MePEG-OPSS-2.5k, and MePEG-OPSS-5k with $T117C_7$ could be fitted with single exponentials, suggesting that in these cases only a single MePEG becomes attached within the lumen of each pore. This conclusion was also supported by the I_∞/I_0 values for these positions.

Relative Reaction Rates for the Seven Cysteine Mutants

The seven cysteine mutants displayed a wide range of reactivity towards the MePEG-OPSS reagents (Tables I and II). Therefore, to estimate the effect of polymer mass on reactivity, k′ values were normalized with respect to the values obtained with MePEG-OPSS-1k, which was assumed to be highly permeant (Fig. 5). When applied from the trans side, MePEG-OPSS-1.8k

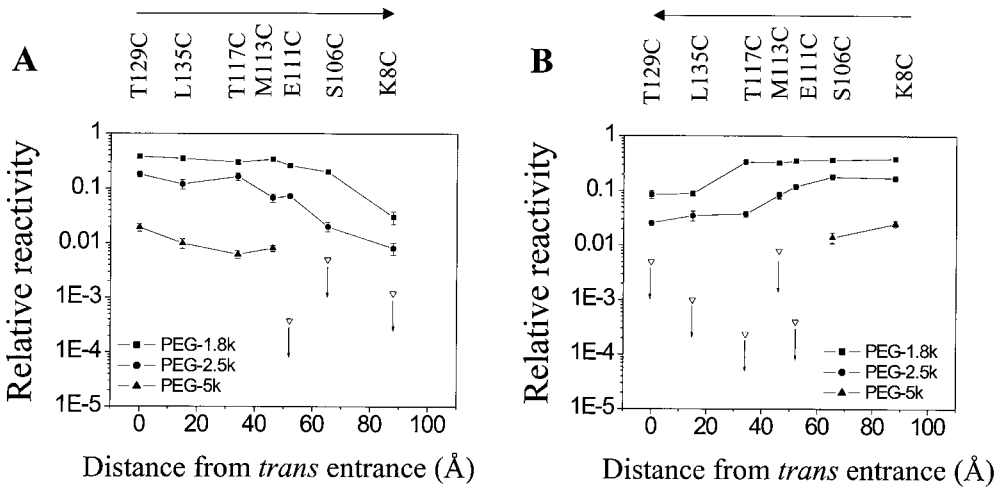

FIGURE 5. Relative reaction rates for seven cysteine mutants with all four MePEG-OPSS reagents. The apparent first-order rate constants (k′, Tables I and II) for the larger reagents were normalized by dividing by the corresponding k′ value for MePEG-OPSS-1k: MePEG-OPSS-1.8k (■), MePEG-OPSS-2.5k (●), and MePEG-OPSS-5k (▲). Mean values (±SD) from four experiments are shown. The open symbols (▽) represent no detectable reaction (see the text) and are placed at a value corresponding to the lowest measurable relative rate. 4 mM MePEG-OPSS was used at pH 8.5. The applied potential was −40 mV, with respect to the trans entrance of the pore. (A) The reagents were applied to the trans side. (B) The reagents were applied to the cis side.

reacted at almost the same normalized rate throughout the entire lumen, until the rate dropped off at the cis entrance (Fig. 5 A). A similar pattern was observed for MePEG-OPSS-2.5k. By contrast, the rate of modification by MePEG-OPSS-5k dropped dramatically at position 111, where reaction was undetectable. Reaction was also undetectable at positions 106 and 8, which lie beyond 111 (Fig. 1). However, it should be noted that the lowest detectable absolute rates at positions 106 and 8 would not produce lowered relative rates as dramatic as that seen at position 111, where the cysteine is highly reactive (Fig. 5 A). In other words, because Cys-111 is very reactive towards MePEG-OPSS-1k (Tables I and II), we were able to estimate that MePEG-OPSS-5k is at least 2,600-fold less reactive than MePEG-OPSS-1k at this position based on the lowest measurable rate (see above). The rate is at least 19-fold lower than expected based on extrapolation of the rates of reaction of MePEG-OPSS-5k at positions 117 and 113. Because of their intrinsically low rates of reaction, the failure to detect a reaction at 106 and 8 with MePEG-OPSS-5k cannot be interpreted with certainty to reflect a lack of accessibility of the reagent.

When the MePEG-OPSS reagents were applied to the cis side, the 1.8- and 2.5-kD reagents also reacted throughout the channel lumen (Fig. 5 B). A complementary pattern of reactivity was seen with MePEG-OPSS-5k when compared with the trans application. MePEG-OPSS-5k reacted with Cys-8 at the trans entrance and Cys-106 in the cavity, but reaction at position 111 was again undetectable. The lack of reaction at position 117, which is highly reactive towards MePEG-OPSS-1k was also diagnostic for greatly reduced accessibility to MePEG-OPSS-5k presented from the cis side. The rates at positions 111 and 117 were at least 50- and 85-fold lower, respectively, than expected based on extrapolation of the rates of reaction of MePEG-OPSS-5k at positions 8 and 106. Although no reaction was detected at positions 113, 135, and 129, the low intrinsic reactivity at these positions renders them less useful for determining accessibility (Fig. 5 B).

Residual Currents with PEGs Tethered at Different Sites in the Lumen

The residual currents (I_∞/I_0) after reaction with the MePEG-OPSSs were determined for the seven cysteine mutants (Fig. 6). Reaction at the cis and trans entrances (positions 8 and 129) produced a modest decrease in conductance to I_∞/I_0 = 0.80–0.95, even though all seven cysteine residues react in these two cases. At position 106 within the cavity, the decrease in conductance was also small, I_∞/I_0 = 0.80–0.90, whether only one MePEG chain was attached (1.8, 2.5, and 5.0 kD) or three (1.0 kD). By contrast, a reaction within the β barrel produced a decrease to I_∞/I_0 = 0.25–0.45. The effect at position 135 was significantly weaker than that at the other three positions in the barrel. Interestingly, the mass of the MePEG chain had little effect on I_∞/I_0.

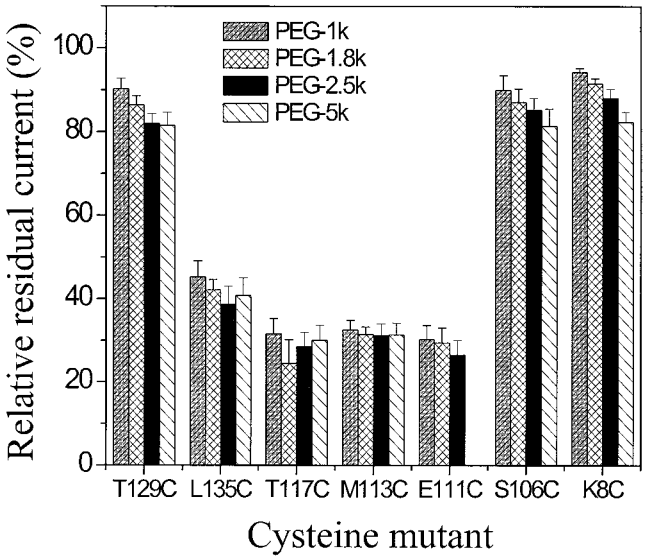

FIGURE 6. Residual currents after the attachment of MePEG in the lumen of the pore. I_∞/I_0 values are shown (n = 4; ±SD). In the cases of MePEG-OPSS-1k, MePEG-OPSS-1.8k, and MePEG-OPSS-2.5k, the reagents were reacted from the trans side. In the case of MePEG-OPSS-5k, modification at positions 129, 135, 117, and 113 was from the trans side, and modification at positions 106 and 8 was from the cis side. MePEG-OPSS-5k does not react at position 111. The values quoted are for attachment of a single MePEG molecules at positions 135, 117, 113, and 111. In the case of position 106, one MePEG is also attached except with MePEG-OPSS-1k, where three sulfhydryls reacted. In the cases of positions 129 and 8, seven residues are modified with all four reagents.

DISCUSSION

The purpose of the present study was to determine whether a set of neutral polymeric sulfhydryl-directed reagents might be used to determine the geometry of the lumen of a transmembrane protein pore. The test protein was staphylococcal αHL, which forms a heptameric pore of known 3-D structure. Specifically, it was hoped that the approach would reveal the location and dimensions of an internal constriction in the lumen of the pore. A set of seven single cysteine mutants of αHL was used in which the mutations were placed along the length of the lumen (Fig. 1). The rates of reaction of each mutant with four reagents with masses of 1.0, 1.8, 2.5, and 5.0 kD were determined. The reagents were applied from both the trans and cis entrances of the pore in separate experiments.

We found that the cysteine mutants exhibited a wide range of reactivities. Therefore, the rates at each position were normalized to the rate observed with the 1.0-kD reagent. Presumably the different reactivities resulted from differences in the local environment of

each cysteine (Holmgren et al., 1996; Pascual and Karlin, 1998; Lu et al., 1999). Because sulfhydryls in their deprotonated forms react with pyridyl disulfides (Brocklehurst and Little, 1970, 1973), the affects of the microenvironment on the pK_a of each cysteine residue must be of importance in determining reactivity. Further, bulky residues near a cysteine would be expected to decrease the rate of reaction, in this case through steric effects. Position 129, at the trans turn of the β barrel, was surprisingly unreactive, suggesting that it is located close to the membrane surface where local pH, steric effects, and surface charge affect reactivity.

The relative rates of reaction at each position were plotted against the distance from the trans entrance of the pore (Fig. 5). First, it is clear that all four reagents can penetrate both the trans and cis entrances. The dependence of the rates of reaction on the mass of the polymers reflects the dimensions of the lumen, as will be shown elsewhere (Movileanu, L., manuscript in preparation). In the present work, we focus on discontinuities in the relative reaction rates as a function of the distance from an entrance. Whether they are applied to the trans or cis entrance, the lower mass polymers of 1.8 and 2.5 kD show similar rates of reaction within the lumen relative to the rates of the 1-kD reagent. By contrast, the 5.0-kD polymer reacts only at positions 129, 135, 117, and 113 when applied from the trans entrance. At positions further from the trans entrance (positions 111, 106, and 8), no reaction can be detected. When applied from the cis entrance, the 5.0-kD polymer reacts at positions 8 and 106, but not at 111, 113, 117, 135, and 129. These results suggest that there is a constriction near position 111, through which the 5-kD reagent cannot pass. Examination of the crystal structure of heptameric αHL (Song et al., 1996; Fig. 1) suggests that the constriction arises from bulky amino acid side chains, notably those of Lys-147, as the polypeptide backbone in the barrel generates a cylinder of almost uniform cross-section. We suggest that reagent in a chamber of the bilayer apparatus is in equilibrium with the solution in the lumen before the constriction. Beyond the constriction, there is a steady-state concentration of reagent determined by the rate of flux into the distal chamber, where the concentration of the reagent is initially zero and always negligible.

Several additional results are incidental to the main findings concerning the location and dimensions of the constriction. The stark contrast between reaction rates at specific residues depending on whether MePEG-OPSS-5k is presented from the trans or the cis side of the protein (e.g., at position 117, Fig. 3 c) shows that αHL is in a single orientation in the bilayer. The similar reaction rates at specific positions for each lower mass polymer whether presented from the trans or cis entrance confirms that the polymers are neutral species at pH 8.5. The mean k'_{trans} for MePEG-OPSS-1k for all residues except those at the entrances (positions 129 and 8) is 0.50 s^{-1}. The corresponding mean k'_{cis} value is 0.51 s^{-1}. Charged polymers would be expected to react at different rates from each side in the same transmembrane potential. The finding that the lower mass polymers presented at the trans entrance react at the cis entrance (and vice versa) shows that the neutral polymers pass through the pore, which was not demonstrated in earlier work using bilayer recording (Krasilnikov et al., 1992; Bezrukov and Vodyanoy, 1993; Bezrukov et al., 1994, 1996; Bezrukov and Kasianowicz, 1997; Bezrukov, 2000), although transport and osmotic protection experiments did show this (Füssle et al., 1981; Palmer et al., 1993). Finally, the results show that a flexible neutral polymer of 5 kD, with a hydrodynamic radius of 22.5 Å (Krasilnikov et al., 1992), which is greater than the radii of the channel entrances (trans, ~10 Å; and cis, ~15 Å), can penetrate into the lumen of the pore.

Once covalently attached, the polymers affect the conductance of the αHL pores (Fig. 6). Single polymers attached in the narrower part of the lumen have a greater effect on conductance than polymers attached at the entrances or in the cis cavity. Therefore, this measurement provides a separate means by which to determine pore geometry. Rather than define the position of a constriction, the conductance measurements appear to afford a rough estimate of relative diameter in the vicinity of the site of attachment: the narrower the diameter, the greater the effect of polymer attachment on conductance. Interestingly, the extent of block is largely independent of the mass of the polymer. In the cases of the residues in the barrel, 135, 117, 113, and 111, the attached polymer may be extruded through the trans entrance, in which case the block would result from the segment remaining in the barrel and the lack of dependence on mass would be reasonable. In the case of position 106, we know that a 5-kD polymer is at least partly extruded from the lumen, on the basis of gel shift experiments (Howorka et al., 2000; Movileanu et al., 2000). A 3.4-kD polymer at position 106 also spends a substantial fraction of time in the cis aqueous phase (Movileanu et al., 2000). Therefore, the similar block observed with the four polymers at position 106 may also be rationalized by the proposition that in each case a segment of similar length is present in the lumen, in this case in the cavity rather than the barrel. Polymer attached at the entrances is presumably largely in the aqueous phase, explaining the low extents of block at positions 129 and 8.

Polymers have been used to size pores in previous studies, several of which have involved single channel measurements. In most cases, the polymers have been applied simultaneously to both sides of the lipid bilayer and, in the cases of αHL, the results have indicated that

PEGs of ~2 kD can partition into the channel lumen to a sufficient extent to produce a marked decrease in conductance and/ or excess channel noise (Krasilnikov et al., 1992; Bezrukov and Vodyanoy, 1993; Bezrukov et al., 1994, 1996; Bezrukov and Kasianowicz, 1997; Bezrukov, 2000). The movement of nucleic acids through the αHL pore also has been demonstrated (Kasianowicz et al., 1996). The effective diameter of the pore can be gauged from its ability to transport single-stranded but not double-stranded DNA, which has a diameter of ~20 Å (Kasianowicz et al., 1996). These previous findings are generally consistent with the results presented here.

Only recently has the internal geometry of pores been approached by the use of inert neutral polymers. Krasilnikov and colleagues determined the diameters of both entrances and the sites of constrictions in the voltage-dependent anion channel (Carneiro et al., 1997), colicin Ia (Krasilnikov et al., 1998), and staphylococcal α-hemolysin (Merzlyak et al., 1999). In these experiments, the unitary conductance was examined before and after the application of a penetrating polymer to one side of the bilayer and a nonpenetrating polymer to the other side. This approach requires the use of high concentrations of polymers (20% in the studies cited), which has several disadvantages including the following: effects on solution conductivity and ionic activity (including changes in access resistance); the generation of streaming potentials; osmotic stress on the protein under investigation (Zimmerberg and Parsegian, 1986); the relatively poor understanding of polymer physics in the semi-dilute regime (where polymer–polymer interactions are significant); and possible interference by impurities in the polymer. Despite these reservations, the findings of Merzlyak and colleagues are also largely consistent with our results.

The present approach, in which far lower concentrations of polymers are used (0.4–2% [wt/vol]) is based on previous studies in which the topologies of ion channels were mapped with low molecular mass sulfhydryl reagents (Akabas et al., 1992; Holmgren et al., 1996; Horn, 1998; Karlin and Akabas, 1998). For example, Wilson and Karlin (1998) located the gate in the nicotinic acetylcholine receptor, which is opened and closed by activating ligands, by reaction with small methanethiosulfonate reagents. A second advantage of our approach is that macroscopic currents are used, although single channel recordings can provide additional information. The need for extensive mutagenesis is certainly a disadvantage. Nevertheless, comprehensive cysteine mutagenesis is often the first order of the day when a new channel or pore is discovered, so this drawback may be less severe than appears at first sight. In addition, the approach may be difficult to implement in the absence of a 3-D structure, yet with a structure it provides little additional information, in most circumstances. However, the advent of better protein folding programs, especially for membrane proteins, and the increasing availability of prototypical membrane protein structures diminish the severity of this limitation by providing testable predictions. In the case of αHL homoheptamers, the presence of seven sulfhydryls led to complications (described above) that would not arise in other situations. However, even in the case of proteins such as αHL, the difficulties can be surmounted by the use of artificial heteromers containing single cysteine residues (Gouaux et al., 1994; Braha et al., 1997; Cheley, S., unpublished work). By contrast, with the present approach, the use of inert polymers requires no mutagenesis and provides data on the wild-type protein rather than mutant forms (Merzlyak et al., 1999).

Our data suggest that polymeric sulfhydryl-directed reagents will be useful for determining the internal geometry of transmembrane protein pores. The reagents might be applied to a variety of pores including additional pore-forming toxins, the outer membrane porins of gram-negative bacteria and components of the immune system such as perforin and the membrane–attack complex of complement. Interesting targets would be pores that open and close, e.g., translocons (Johnson and van Waes, 1999; Andrews, 2000) and gap junctions (Nicholson and Bruzzone, 1997; Unger et al., 1999). The reagents might also be used to examine the vestibules of ligand- and voltage-gated ion channels (Doyle et al., 1998; Miyazawa et al., 1999). We have also shown that a quantitative analysis of the rates of modification by the MePEG-OPSS reagents can provide a quite accurate estimate of the diameter of the transmembrane barrel of αHL (Movileanu, L., manuscript in preparation). Even at this point, it is clear that additional reactive polymers will be useful in studies of this kind; e.g., flexible polymers with different persistence lengths, more rigid polymers approximating hard spheres, and polymers that provide a range of reactivity towards sulfhydryl groups. Information from fundamental studies such as that presented here might also be applied to more elaborate investigations such as those with functionalized polymers (Kramer and Karpen, 1998; Blaustein et al., 2000; Movileanu et al., 2000).

We thank Sean Conlan for help with molecular modeling.

This work was supported by grants from the US Department of Energy, the National Institutes of Health, and Office of Naval Research (MURI-1999) to H. Bayley, and the Air Force Office of Scientific Research (MURI-1998). S.H. holds a postdoctoral fellowship from the Austrian Science Foundation (Fonds zur Förderung der wissenschaftlichen Forschung).

Submitted: 3 November 2000
Revised: 2 January 2001
Accepted: 3 January 2001

REFERENCES

Akabas, M.H., D.A. Stauffer, M. Xu, and A. Karlin. 1992. Acetylcho-

line receptor channel structure probed in cysteine-substitution mutants. *Science.* 258:307–310.

Andrews, D.W. 2000. Transport across membranes: a question of navigations. *Cell.* 102:139–144.

Bevans, C.G., M. Kordel, S.K. Rhee, and A.L. Harris. 1998. Isoform composition of connexin channels determines selectivity among second messengers and uncharged molecules. *J. Biol. Chem.* 273: 2808–2816.

Bezrukov, S.M. 2000. Ion channels as molecular Coulter counters to probe metabolite transport. *J. Membr. Biol.* 174:1–13.

Bezrukov, S.M., and J.J. Kasianowicz. 1997. The charge state of an ion channel controls neutral polymer entry into its pore. *Eur. Biophys. J.* 26:471–476.

Bezrukov, S.M., and I. Vodyanoy. 1993. Probing alamethicin channels with water-soluble polymers. Effect on conductance of channel states. *Biophys. J.* 64:16–25.

Bezrukov, S.M., I. Vodyanoy, R.A. Brutyan, and J.J. Kasianowicz. 1996. Dynamics and free energy of polymer partitioning into a nanoscale pore. *Macromolecules.* 29:8517–8522.

Bezrukov, S.M., I. Vodyanoy, and V.A. Parsegian. 1994. Counting polymers moving through a single ion channel. *Nature.* 370:279–281.

Blaustein, R.O., P.A. Cole, C. Williams, and C. Miller. 2000. Tethered blockers as molecular "tape measures" for a voltage-gated K^+ channel. *Nat. Struct. Biol.* 7:309–311.

Braha, O., B. Walker, S. Cheley, J.J. Kasianowicz, L. Song, J.E. Gouaux, and H. Bayley. 1997. Designed protein pores as components for biosensors. *Chem. Biol.* 4:497–505.

Brocklehurst, K., and G. Little. 1970. A novel reactivity of papain and a convenient active site titration on the presence of other thiols. *FEBS Lett.* 9:113–116.

Brocklehurst, K., and G. Little. 1973. Reactions of papain and low-molecular weight thiols with some aromatic disulphides. *Biochem. J.* 133:67–80.

Carneiro, C.M.M., O.V. Krasilnikov, L.N. Yuldasheva, A.C. Campos de Carvalho, and R.A. Nogueira. 1997. Is the mammalian porin channel, VDAC, a perfect cylinder in the high conductance state. *FEBS Lett.* 416:187–189.

Cheley, S., O. Braha, X. Lu, S. Conlan, and H. Bayley. 1999. A functional protein pore with a "retro" transmembrane domain. *Protein Sci.* 8:1257–1267.

Christopher, J.A. 1998. SPOCK: The Structural Properties Observation and Calculation Kit (program manual). Center for Macromolecular Design, Texas A&M University, College Station, TX.

Colombini, M. 1980. Pore size and properties of channels from mitochondria isolated from *Neurospora crassa. J. Membr. Biol.* 53:79–84.

Decad, G.M., and H. Nikaido. 1976. Outer membrane of gram-negative bacteria. XII. Molecular sieving function of cell wall. *J. Bacteriol.* 128:325–336.

Doyle, D.A., J.M. Cabral, R.A. Pfuetzner, A. Kuo, J.M. Gulbis, S.L. Cohen, B.T. Chait, and R. MacKinnon. 1998. The structure of the potassium channel: molecular basis of K^+ conduction and selectivity. *Science.* 280:69–77.

Fajardo, D.A., J. Cheung, C. Ito, E. Sugawara, H. Nikaido, and R. Misra. 1998. Biochemistry and regulation of a novel *Escherichia coli* K-12 porin protein, OmpG, which produces unusually large channels. *J. Bacteriol.* 180:4452–4459.

Füssle, R., S. Bhakdi, A. Sziegoleit, J. Tranum-Jensen, T. Kranz, and H.-J. Wellensiek. 1981. On the mechanism of membrane damage by *Staphylococcus aureus* α-toxin. *J. Cell Biol.* 91:83–94.

Gouaux, J.E., O. Braha, M.R. Hobaugh, L. Song, S. Cheley, C. Shustak, and H. Bayley. 1994. Subunit stoichiometry of staphylococcal α-hemolysin in crystals and on membranes: a heptameric transmembrane pore. *Proc. Natl. Acad. Sci. USA.* 91:12828–12831.

Gu, L.-Q., O. Braha, S. Conlan, S. Cheley, and H. Bayley. 1999. Stochastic sensing of organic analytes by a pore-forming protein containing a molecular adapter. *Nature.* 398:686–690.

Hamman, B.D., J.-C. Chen, E.E. Johnson, and A.E. Johnson. 1997. The aqueous pore through the translocon has a diameter of 40-60 Å during cotranslational protein translocation at the ER membrane. *Cell.* 89:535–544.

Hille, B. 1992. Ionic Channels of Excitable Membranes. 2nd ed. Sinauer Associates, Inc., Sunderland, MA. 607 pp.

Holmgren, M., Y. Liu, Y. Xu, and G. Yellen. 1996. On the use of thiol-modifying reagents to determine channel topology. *Neuropharmacology.* 35:797–804.

Holz, R., and A. Finkelstein. 1970. The water and nonelectrolyte permeability induced in thin lipid membranes by the polyene antibiotics nystatin and amphotericin B. *J. Gen. Physiol.* 56:125–145.

Horn, R. 1998. Explorations of voltage-dependent conformational changes using cysteine scanning. *Methods Enzymol.* 293:145–155.

Howorka, S., L. Movileanu, X. Lu, M. Magnon, S. Cheley, O. Braha, and H. Bayley. 2000. A protein pore with a single polymer chain tethered within the lumen. *J. Am. Chem. Soc.* 122:2411–2416.

Johnson, A.E., and M.A. van Waes. 1999. The translocon: a dynamic gateway at the ER membrane. *Annu. Rev. Cell Dev. Biol.* 15:799–842.

Karlin, A., and M. Akabas. 1998. Substituted-cysteine accessibility method. *Methods Enzymol.* 293:123–145.

Kasianowicz, J.J., E. Brandin, D. Branton, and D.W. Deamer. 1996. Characterization of individual polynucleotide molecules using a membrane channel. *Proc. Natl. Acad. Sci. USA.* 93:13770–13773.

Korchev, Y.E., C.L. Bashford, G.M. Alder, J.J. Kasianowicz, and C.A. Pasternak. 1995. Low conductance states of a single ion channel are not 'closed'. *J. Membr. Biol.* 147:233–239.

Kramer, R.H., and J.W. Karpen. 1998. Spanning binding sites on allosteric proteins with polymer-linked ligand dimers. *Nature.* 395: 710–713.

Krasilnikov, O.V., R.Z. Sabirov, V.I. Ternovsky, P.G. Merzliak, and J.N. Muratkhodjaev. 1992. A simple method for the determination of the pore radius of ions channels in planar lipid bilayer membranes. *FEMS Microbiol. Immunol.* 105:93–100.

Krasilnikov, O.V., J.B. Da Cruz, L.N. Yuldasheva, W.A. Varanda, and R.A. Nogueira. 1998. A novel approach to study the geometry of the water lumen of ion channels: colicin Ia channels in planar lipid bilayers. *J. Membr. Biol.* 161:83–92.

Krishnasastry, M., B. Walker, O. Braha, and H. Bayley. 1994. Surface labeling of key residues during assembly of the transmembrane pore formed by staphylococcal α-hemolysin. *FEBS Lett.* 356:66–71.

Laemmli, U.K. 1970. Cleavage of structural proteins during the assembly of the head of bacteriophage T4. *Nature.* 227:680–685.

Lu, T., B. Nguyen, X. Zhang, and J. Yang. 1999. Architecture of a K^+ channel inner pore revealed by stoichiometric covalent modification. *Neuron.* 22:571–580.

Menestrina, G. 1986. Ionic channels formed by *Staphylococcus aureus* alpha-toxin: voltage-dependent inhibition by divalent and trivalent cations. *J. Membr. Biol.* 90:177–190.

Merzlyak, P.G., L.N. Yuldasheva, C.G. Rodrigues, C.M.M. Carneiro, O.V. Krasilnikov, and S.M. Bezrukov. 1999. Polymeric nonelectrolytes to probe pore geometry: application to the α-toxin transmembrane channel. *Biophys. J.* 77:3023–3033.

Miyazawa, A., Y. Fujiyoshi, M. Stowell, and N. Unwin. 1999. Nicotinic acetylcholine receptor at 4.6 Å resolution: transverse tunnels in the channel wall. *J. Mol. Biol.* 288:765–786.

Montal, M., and P. Mueller. 1972. Formation of bimolecular membranes from lipid monolayers and study of their electrical properties. *Proc. Natl. Acad. Sci. USA.* 69:3561–3566.

Movileanu, L., S. Howorka, O. Braha, and H. Bayley. 2000. Detecting protein analytes that modulate transmembrane movement of a polymer chain within a single protein pore. *Nat. Biotechnol.* 18: 1091–1095.

Nicholson, S.M., and R. Bruzzone. 1997. Gap junctions: getting the

message through. *Curr. Biol.* 7:R340–R344.

Palmer, M., U. Weller, M. Messner, and S. Bhakdi. 1993. Altered pore-forming properties of proteolytically nicked staphylococcal α-toxin. *J. Biol. Chem.* 268:11963–11967.

Pascual, J.M., and A. Karlin. 1998. State-dependent accessibility and electrostatic potential in the channel of the acetylcholine receptor-inferences from the rates of reaction of thiosulfonates with substituted cysteines in the M2 segment of the alpha subunit. *J. Gen. Physiol.* 111:717–739.

Scherrer, R., and P. Gerhardt. 1971. Molecular sieving by the *Bacillus megaterium* cell wall and protoplast. *J. Bacteriol.* 107:718–735.

Schwab, J.C., C.J.M. Beckers, and K.A. Joiner. 1994. The parasitophorous vacuole membrane surrounding intracellular *Toxoplasma gondii* functions as a molecular sieve. *Proc. Natl. Acad. Sci. USA.* 91:509–513.

Song, L., M.R. Hobaugh, C. Shustak, S. Cheley, H. Bayley, and J.E. Gouaux. 1996. Structure of staphylococcal α-hemolysin, a heptameric transmembrane pore. *Science.* 274:1859–1865.

Szabò, I., G. Bàthori, F. Tombola, M. Brini, A. Coppola, and M. Zoratti. 1997. DNA translocation across planar bilayers containing *Bacillus subtilis* ion channels. *J. Biol. Chem.* 272:25275–25282.

Szabò, I., G. Bàthori, F. Tombola, A. Coppola, I. Schmehl, M. Brini, A. Ghazi, V. De Pinto, and M. Zoratti. 1998. Double-stranded DNA can be translocated across a planar bilayer containing purified mitochondrial porin. *FASEB J.* 12:495–502.

Unger, V.M., N.M. Kumar, N.B. Gilula, and M. Yeager. 1999. Three-dimensional structure of a recombinant gap junction membrane channel. *Science.* 283:1176–1180.

Vodyanoy, I., and S.M. Bezrukov. 1992. Sizing of an ion pore by access resistance measurements. *Biophys. J.* 62:10–11.

Walker, B., and H. Bayley. 1995. Key residues for membrane binding, oligomerization, and pore-forming activity of staphylococcal α-hemolysin identified by cysteine scanning mutagenesis and targeted chemical modification. *J. Biol. Chem.* 270:23065–23071.

Wilson, G.G., and A. Karlin. 1998. The location of the gate in the acetylcholine receptor. *Neuron.* 20:1269–1281.

Woghiren, C., B. Sharma, and S. Stein. 1993. Protected thiol-polyethylene glycol: a new activated polymer for reversible protein modification. *Bioconjugate Chem.* 4:314–318.

Zimmerberg, J., and V.A. Parsegian. 1986. Polymer inaccessible volume changes during opening and closing of a voltage-dependent ionic channel. *Nature.* 323:36–39.